

Vertical profiles of trace nitrate in surface oceanic waters of the North Pacific Ocean and East China Sea

Jota KANDA¹, Takayuki ITOH² and Motomune NOMURA²

Abstract: Trace nitrate in surface waters at several stations of the North Pacific Ocean and East China Sea were determined by a high-sensitivity chemiluminescence method. The detailed vertical distribution of nitrate within the surface layer based on water samples taken at small depth intervals revealed that nitrate concentrations were approximately uniform within the euphotic zone, then increased abruptly with depth from the upper end of the nitracline. Nitrate concentrations above the nitracline ranged 3.1–96.2nM, likely reflecting nitrate supply from depths. The depth of the upper end of the nitracline was located at a light depth of 0.58–3.5% at all stations except two, at which the surface mixed layer extended down to the upper end of the nitracline. These depths corresponded closely to the conventional bottom of the euphotic zone, indicating a strong biological control on the nitrate distribution. If the observed nitrate distribution is maintained steadily, net biological nitrate consumption should occur over a narrow depth range near the upper end of the nitracline and no net uptake or regeneration should occur in the upper layers of the euphotic zone.

Keywords: Nitrate, Vertical profile, Chemiluminescent technique

1. Introduction

Nitrate in the surface layer of stratified ocean waters is depleted by biological consumption to levels substantially below 100nM. However, as the detection limits of conventional spectrophotometric analysis for nitrate are usually in the range of 100nM (STRICKLAND and PARSONS, 1972), alternative techniques capable of much lower detection limits are required. The use of chemiluminescence for high-sensitivity analysis of nitrate (GARSDALE, 1982) revealed the presence of trace nitrate in the low nanomolar range at sites in oligotrophic waters (GARSDALE, 1985; EPPLEY and RINGER, 1986). Other high-sensitivity analytical methods are now also in use (OUDOT and MONTEL, 1989; ZHANG, 2000).

These high-sensitivity analytical methods

have been used to determine nitrate concentrations in several oceanic domains (e.g. GARSDALE, 1985; EPPLEY and RINGER, 1986; GLOVER *et al.*, 1988; EPPLEY *et al.*, 1990; WOODWARD and OWENS, 1990; MANTOURA *et al.*, 1993; HARRISON *et al.*, 1996; DORE and KARL, 1996a; LIPSCHULTZ, 2001; CAVENDER-BARES *et al.*, 2001; KANDA *et al.*, 2003; CHEN *et al.*, 2004; KROM *et al.*, 2005). However, high-sensitivity measurements of the nitrate distribution remain limited, particularly for the western part of the Pacific Ocean. In the present paper, a modified chemiluminescence technique following GARSDALE (1982) is employed to obtain detailed vertical profiles of nitrate concentration at several sites in the Pacific Ocean and in the waters adjacent to Japan. The obtained results are discussed with regard to the physical structure of the water column and the biological processes relevant to the control of nitrate concentrations. Emphasis is placed on the detailed variation of nitrate near the upper end of the nitracline, where nitrate concentrations begin to increase sharply with depth.

¹ Faculty of Marine Science, Tokyo University of Marine Science and Technology, 4-5-7 Konan, Minato-ku, Tokyo 108-8477, JAPAN

² Faculty of Science, Shizuoka University, 836 Ohya, Suruga-ku, Shizuoka-shi, Shizuoka 422-8529, JAPAN

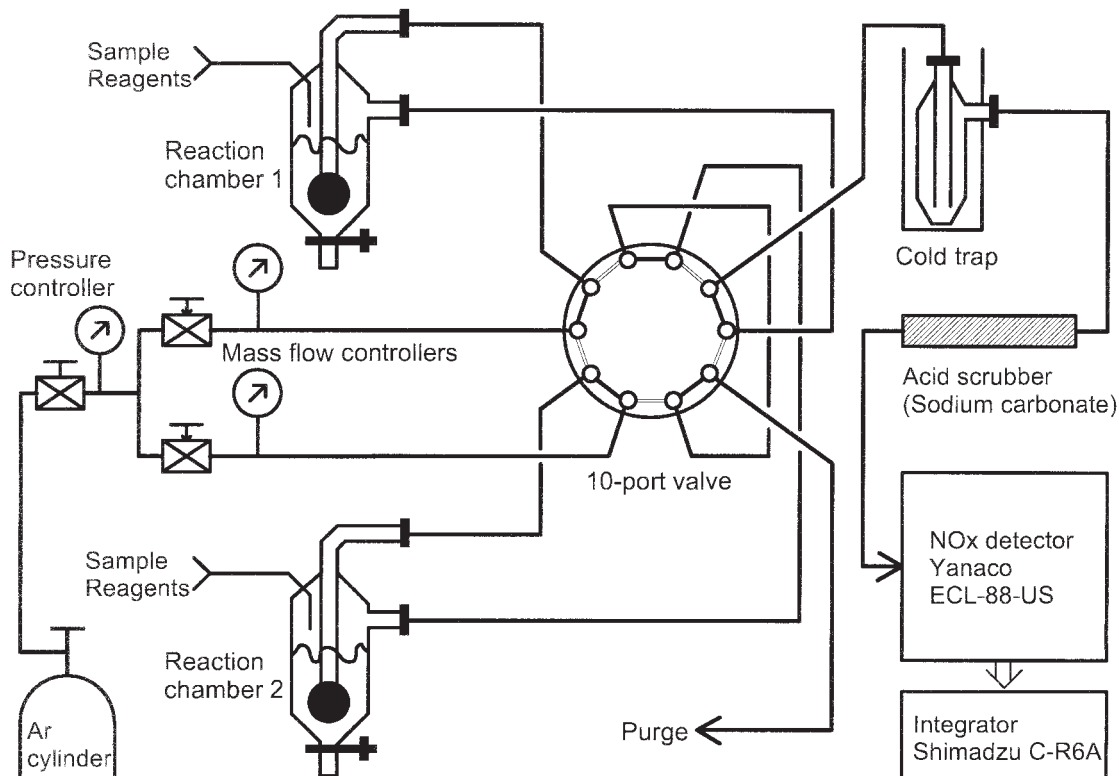


Fig. 1. Schematic diagram of chemiluminescent analysis.

2. Materials and Methods

Nitrate concentrations were determined by the chemiluminescent method of GARSIDE (1982) using the analytical system of COX (1980) and GARSIDE (1982) with modifications to increase the sample processing rate. In the present study, a system with two reaction chambers connected via a 10-port valve is used (Fig. 1). The two chambers are used alternately. The carrier gas (Ar) is supplied from a gas cylinder through two different lines; one line is dedicated strictly for analysis and is connected directly to the chemiluminescent NOx detector, and the other line is used for pre-purging with the mixed reducing reagent. The gas flow in each line is controlled by a pressure regulator and a mass-flow controller.

While the chamber is connected to the pre-purge line, the reducing reagents are introduced successively by dispenser units connected to the chamber in the following order: 10mL sulfuric acid (H_2SO_4 , ca. 95%), 2mL 4% (w/v)

aqueous ammonium iron (II) sulfate ($\text{Fe}(\text{NH}_4)_2(\text{SO}_4)_2 \cdot 6\text{H}_2\text{O}$) solution, and 2mL 2% (w/v) aqueous ammonium molybdate ($(\text{NH}_4)_2\text{MoO}_4$) solution. After pre-purging, the line is switched to the analytical line, and 10mL of the seawater sample is introduced to the chamber by a dispenser unit. The evolved nitrogen monoxide (NO) is lead to a chemiluminescent NOx detector (ECL-88US, Yanaco, Kyoto, Japan), and the peak area of NO concentration is calculated by an integrator (C-R6A, Shimadzu, Kyoto, Japan). The peak area was calibrated in advance against the peak area of standard solutions of known concentrations. Another reaction chamber was pre-purged in preparation for analysis of the following sample during analysis of the current sample. The samples and standards were prepared by adding a 1/50 proportion of 1% sulfanilamide solution. The present analysis thus determines only nitrate, not nitrite (GARSIDE, 1982).

Pure water obtained from a water

Table 1. Station locations and date/time of sampling

Station/Cast	Location	Date	Local Time	Cruise
C	22° 46'N, 158° 07'W	31Oct. 1993	10 : 20	KH-93-4
B CastB10	31° 40'N, 136° 00'E	2Sept. 1995	19 : 10	KT-95-12
CastB12		3Sept. 1995	00 : 10	K-95-09
D4	29° 18'N, 127° 28'E	5Nov. 1995	14 : 21	K-95-09
D6	29° 21'N, 127° 21'E	6Nov. 1995	18 : 42	K-95-09
G2	28° 00'N, 126° 45'E	10Nov.1995	16 : 38	K-95-09
G3	28° 01'N, 126° 43'E	12Nov.1995	11 : 58	K-95-09
G4	28° 04'N, 126° 39'E	13Nov.1995	06 : 37	K-95-09

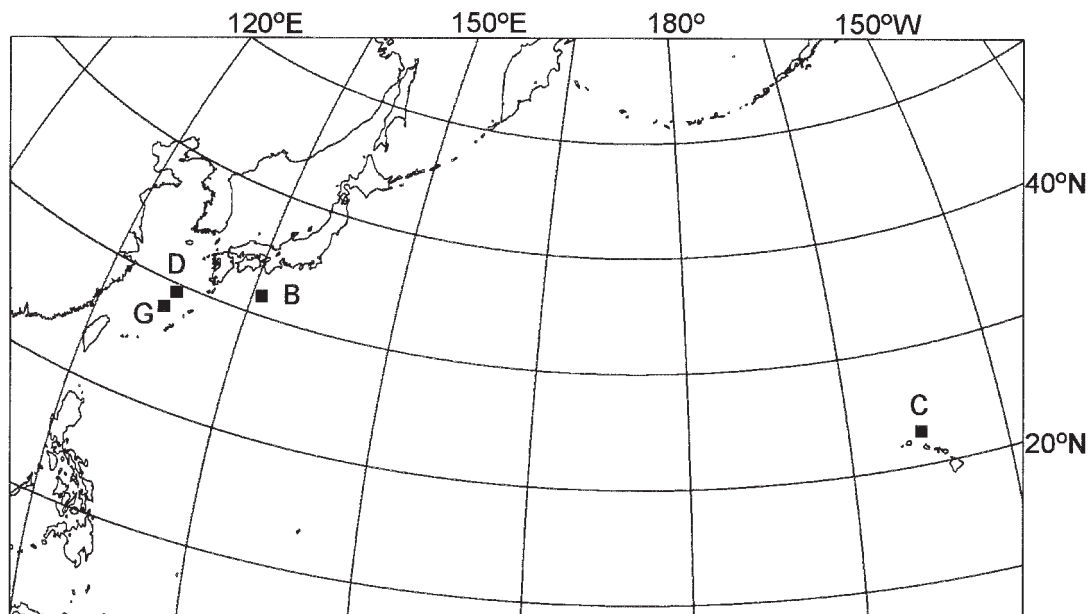


Fig. 2. Station locations.

purification system (Milli-Q Lab, Nihon Millipore, Tokyo, Japan) was used as an analytical blank. The calculated detection limit (y_B+3s_B) for the present analyses is 2.1nM, with reproducibility at 20nM nitrate concentration of 1.8% ($n=10$). All glassware used in the analysis was rinsed with dilute hydrochloric acid solution (ca. 0.05M) and pure water immediately prior to analysis.

Samples for nitrate analysis were obtained during cruises KH-93-4 of the research vessel (R/V) *Hakuho-maru*, KT-95-12 of R/V *Tansei-maru*, and K-95-09 of R/V *Kaiyo* (Table 1). Vertical profiles were obtained from a total of 8 casts at locations shown in Fig. 2. One profile was obtained at Station C of KH-93-4, which is located off Hawaii in the observational area of Station ALOHA of the Hawaiian

Ocean Time-series (KARL and LUKAS, 1996). Station B (KT-95-12) was located in pelagic water south of the Kii Peninsula, Japan, where the 2 casts (B10 and B12) were conducted near sunset and at midnight, respectively. Stations D4, D6, G2, G3 and G6 were in waters off Okinawa, Japan in the shelf-break and trough region of the East China Sea (not on the continental shelf). Stations D4 and D6 were on Line D of the K-95-09 cruise undertaken as part of the MASFLEX project (TSUNOGAI *et al.*, 2003). Stations G2, G3 and G6 were on Line G of the same cruise. These stations were located at intervals of several miles, and only approximate locations are shown (D and G) in Fig. 2. Details of sampling casts are listed in Table 1.

Seawater samples were collected in Niskin bottles using a rosette multi-sampler. Water

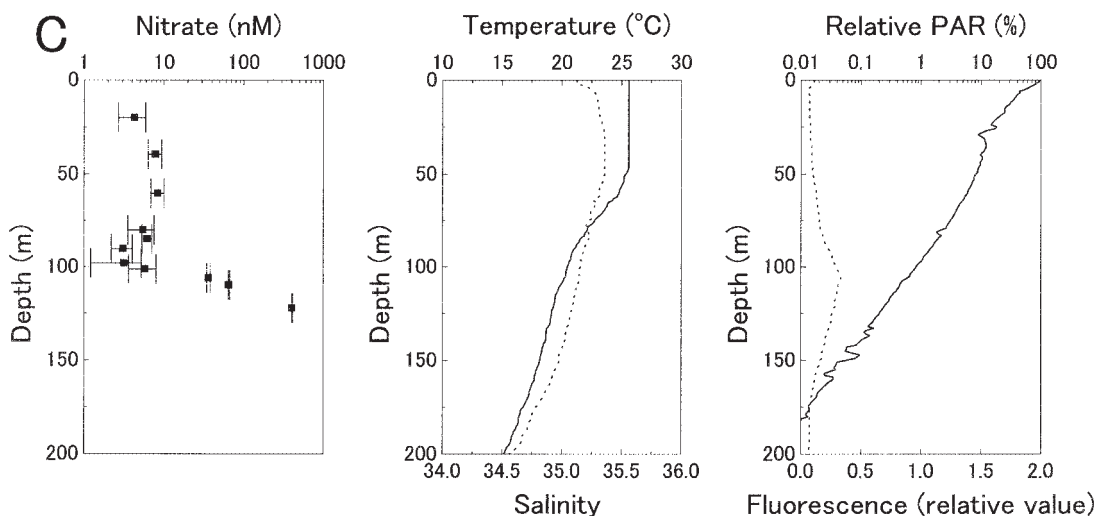


Fig. 3. Vertical profiles of nitrate, temperature, salinity, relative PAR and chlorophyll fluorescence at Station C. Error bars indicate standard deviation of 3 to 8 repeated measurement for one depth sample.

samples were often taken at small depth intervals (down to 5m). While we took care to ascend (descend) the samplers at a rate below ca. 0.3m s^{-1} , possible effect of perturbation by the CTD-sampler system on the observed nitrate distribution should not be precluded. Temperature and salinity profiles were obtained using a Niel-Brown or a Seabird CTD system. Underwater irradiance and chlorophyll fluorescence were observed using either an OCTOPUS system (ISHIMARU et al., 1984) or a natural fluorescence profiler (PNF-300, Biospherical Instruments, San Diego, USA). The underwater irradiance was determined as the photosynthetically available radiation (PAR) scalar irradiance on a quantum basis. The seawater samples were stored frozen until later analysis ashore, except for samples obtained at Station C of KH-93-4, where analysis was performed onboard.

3. Results

Profiles obtained at Station C near Hawaii showed that nitrate concentration ranged from 3.1 to 8.4nM in the upper 100m of the water column and was relatively uniform (Fig. 3). The nitrate concentration at a depth of 101m was 5.8nM, increasing to 36.1 nM at 106m and rising sharply with depth thereafter. The upper end of the nitracline is thus inferred to be

located between 101 and 106m. The surface mixed layer was ca. 50m thick, and the temperature and salinity decreased steadily below this level. The maximum chlorophyll fluorescence occurred at 106m, only a few meters from the upper end of the nitracline. The 1% light depth was 97m, and the upper end of the nitracline corresponded to a light depth of 0.58–0.78%.

At Station B, south of Honshu Island, Japan, two nitrate profiles were obtained at an interval of 5h, and slight differences in the nitrate concentrations and vertical distributions were found (Fig. 4). Nitrate concentrations in the 20–90m interval of the first cast at dusk (B10) and the 50–95m interval of the second cast at midnight (B12) were in the range of 20.1–23.8nM. The upper end of the nitracline was located at 90–95m at the time of B10 and 95–100m for B12. The nitracline depth was thus slightly deeper at midnight. The nitrate concentration increased with depth except for a slight decrease at a 105m in both casts. CTD observations indicate that the mixed layer at dusk (B10) extended to 32m, while that at midnight (B12) extended to 36m. The isotherm depth was also slightly deeper at midnight; the 22.5 °C level occurred at 101m at dusk but at 103m at midnight. Both the chlorophyll maximum and the 1% light depth were located at 101m.

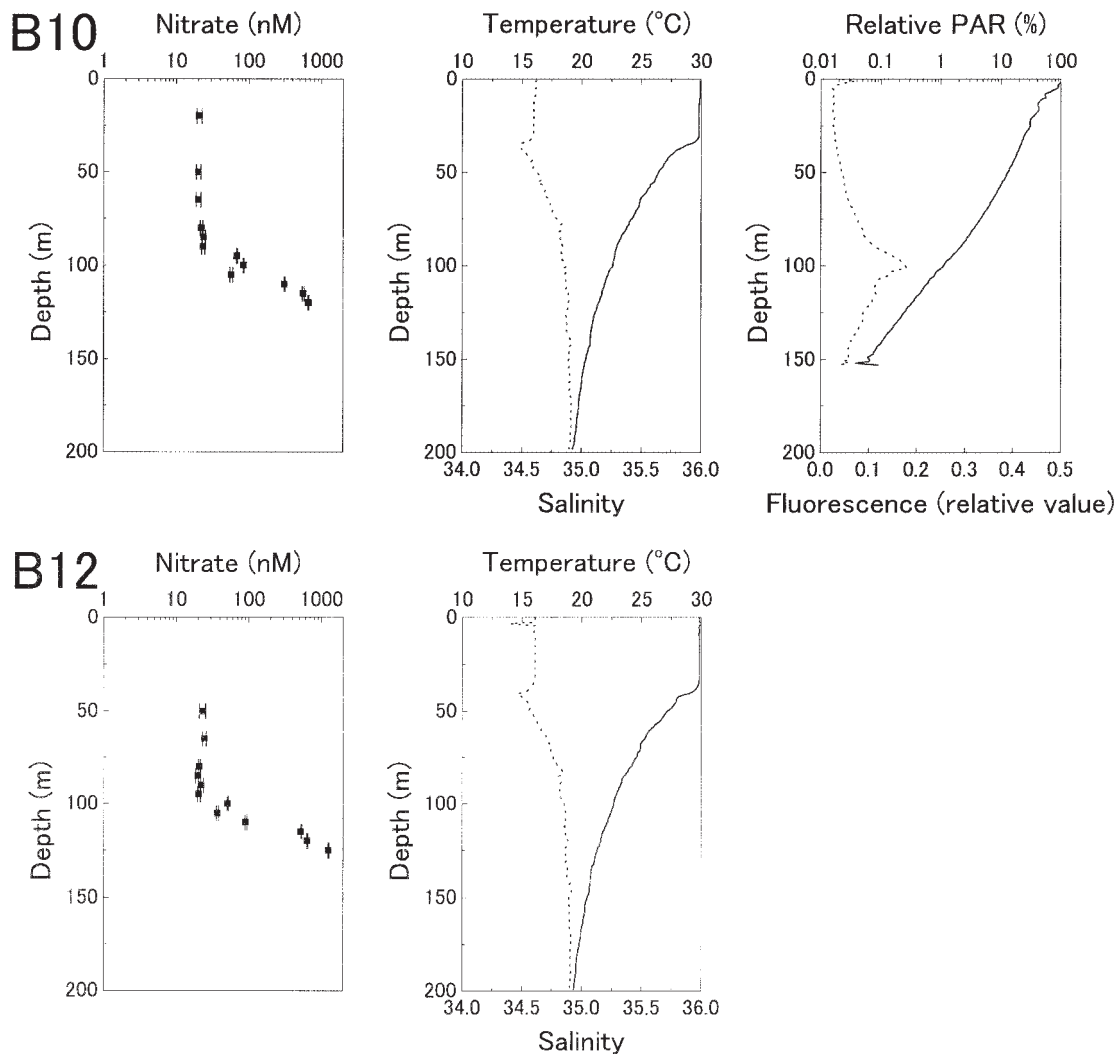


Fig. 4. Vertical profiles of nitrate, temperature and salinity at Station B at dusk (B10, upper) and midnight (B12, lower). Relative PAR and chlorophyll fluorescence were obtained in a separate cast during the daytime (see text).

Note that the observation of chlorophyll fluorescence and underwater irradiance was performed during the daylight hours on the sampling day (Sept. 2, 1995) and thus may not be directly comparable to the profiles observed by the dusk and midnight casts. The upper end of the nitracline (90–100m) was located at a light depth of 1.1–2.1%.

The nitrate concentration in the upper 80m at Station D4 was relatively high, ranging from 35.6 to 96.2nM (Fig. 5). The nitrate distribution was complex. The surface mixed

layer extended to a depth of ca. 40m, and another layer with relatively uniform temperature and salinity was found at depths of 60–90m. Both temperature and salinity were lower in this layer, and the nitrate concentration was also relatively low (35–45nM) in the 60–80m. The nitrate concentration increased from 45.1nM at 80m to 531nM at 90m. The 1% light depth was located at 81m, and the upper end of the nitracline (80–90 m) was located at a light depth of 0.64–1.1%. At Station D6, the surface mixed layer was approximately 60m thick, and

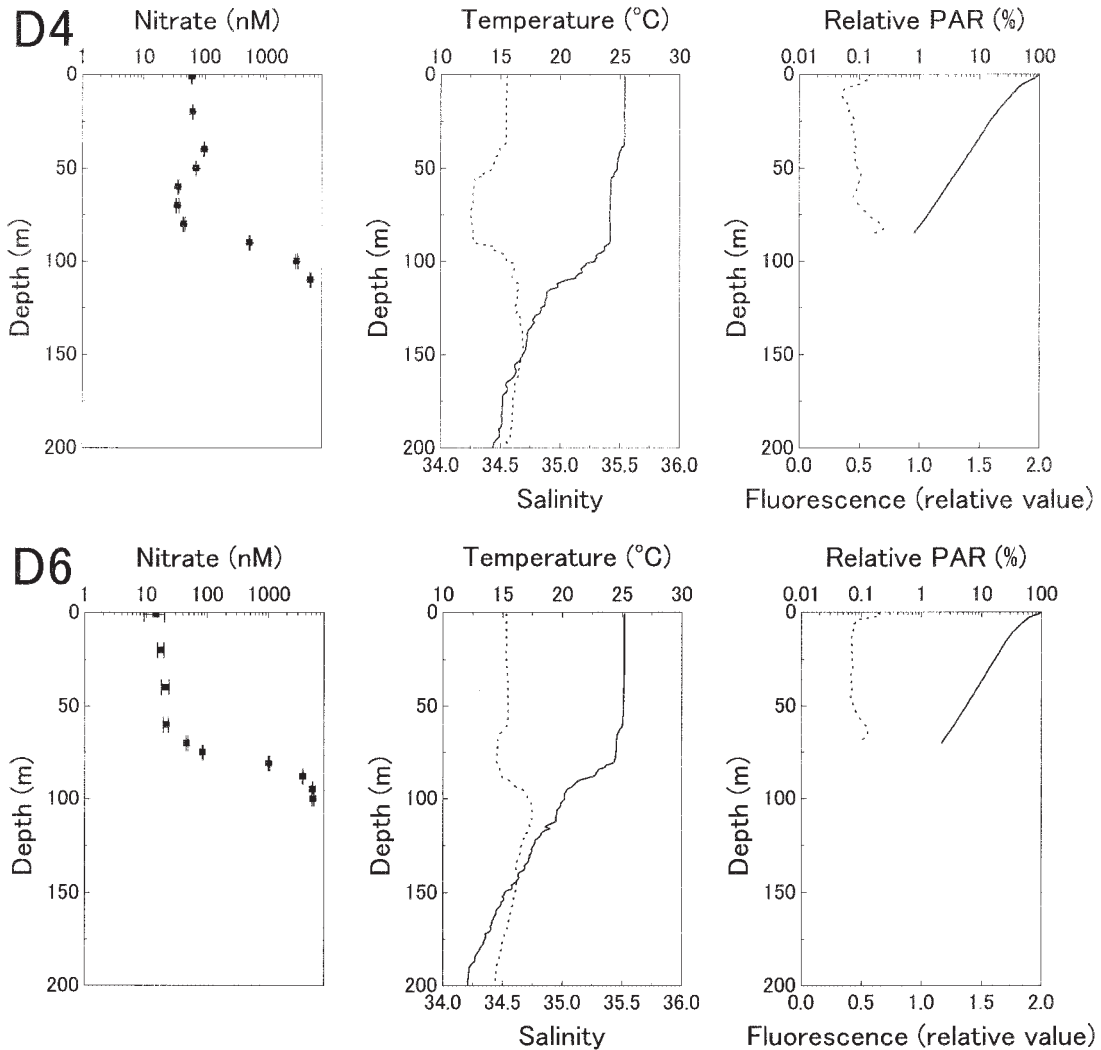


Fig. 5. Vertical profiles of nitrate, temperature, salinity, relative PAR and chlorophyll fluorescence at Stations D4 (upper) and D6 (lower).

a thin layer with uniform temperature and salinity occurred at 70–75m (Fig. 5). The nitrate concentration in the upper 60m of Station D6 was in the range of 14.5–21.3nM. The concentration at 60m was 21.3nM, increasing to 46.3nM at 70m and 83.2nM at 75m. The 1% light depth was outside the observed range of the natural fluorescence profiler, but is inferred by extrapolation to have occurred at a depth of 86m. The upper end of the nitracline (60–70m) corresponded to a light depth of 2.2–3.5%.

At Stations G2, G3 and G6 (Fig. 6), the

surface mixed layer extended deeper, reaching 105m, 85m and 100m, respectively. The nitrate concentrations within these mixed layers ranged from 31.5 to 45.9nM at G2, 24.6–25.7nM at G3, and 25.2–47.1nM at G6. The upper end of the nitracline occurred at a depth of 110–120m at G2, 80–90m at G3, and 90–95m at G6. The 1% light depths were about 93m (by extrapolation) at G2, 98m at G3 and 72m at G6. At G2 and G6, the upper end of the nitracline was much deeper than the 1% light depth, where the upper end of the nitracline at G2 (110–120m) corresponded to a light depth of 0.30–

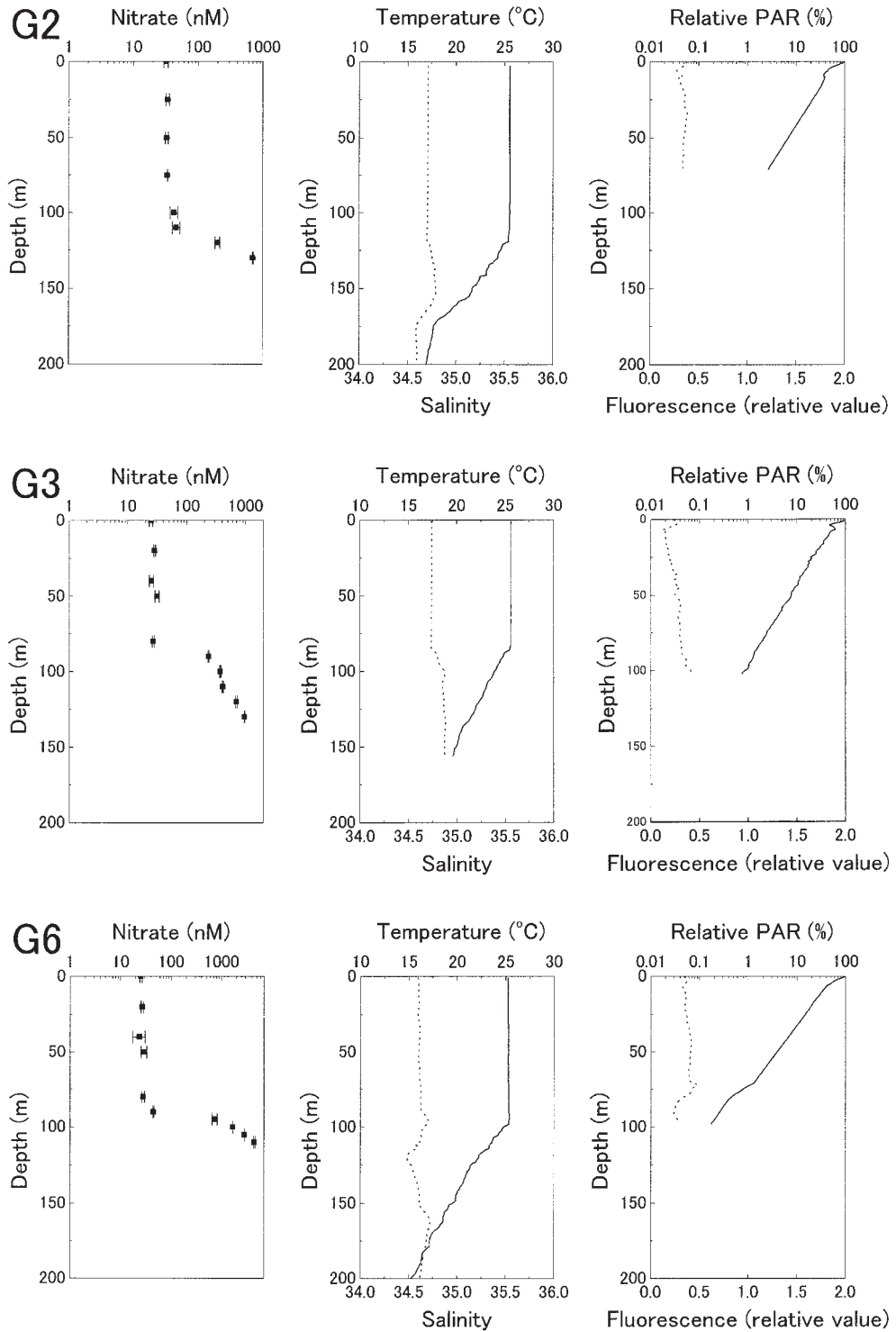


Fig. 6. Vertical profiles of nitrate, temperature, salinity, relative PAR and chlorophyll fluorescence at Stations G2 (upper), G3 (middle) and G6 (lower).

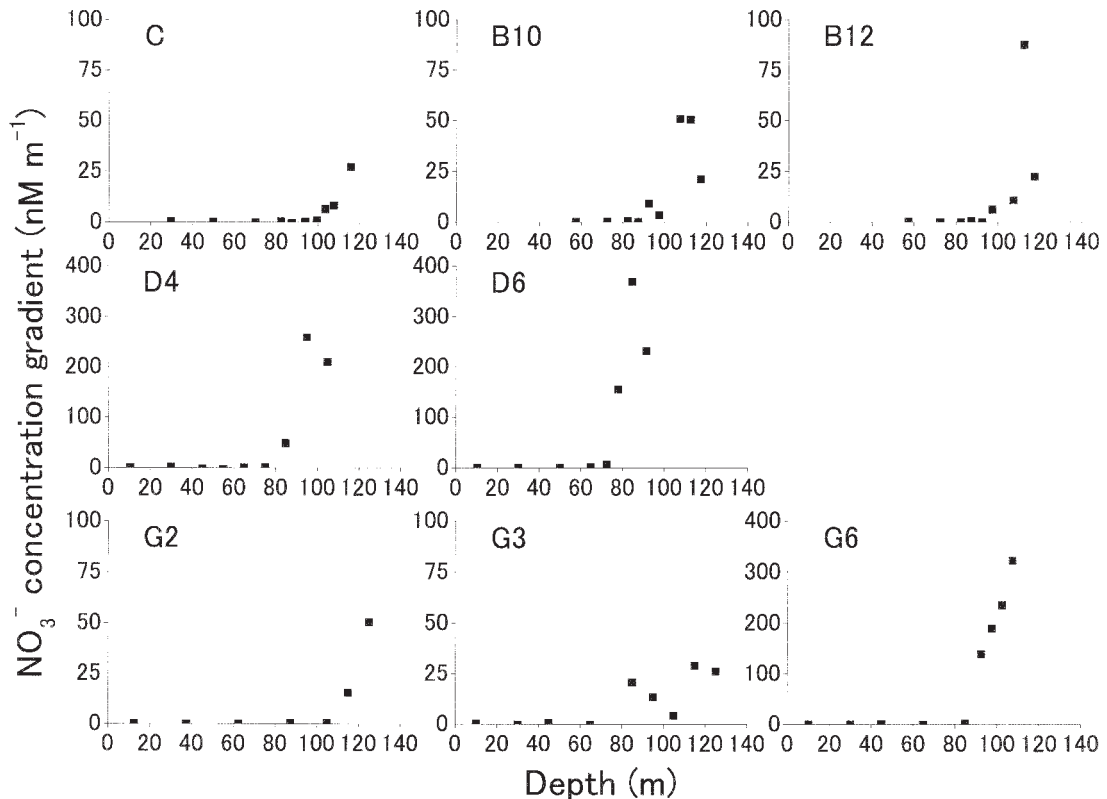


Fig. 7. Variation in nitrate concentration gradient with depth. Difference in nitrate concentration was divided by the depth interval and plotted against the mean depth of two sampling depths. Positive values indicate an increase in concentration with depth.

0.47%, and that at G6 (90–95m) corresponded to a light depth of 0.21–0.26%. In contrast, the upper end of the nitracline at G3 (80–90m) occurred at a light depth of 1.3–2.0%.

4. Discussion

Variation of nitrate concentrations in surface layers

The nitrate concentrations in surface waters of Station C were less than 10nM but still above the detection limit of the present analysis. These low but non-zero values are found consistently at this station in the time series observations of HOT (LETELIER *et al.*, 2000), as well as in other areas of the subtropical oceans (EPPLEY *et al.*, 1990; HARRISON *et al.*, 1996; CAVENDER-BARES *et al.*, 2001). The existence of a threshold concentration of nitrate uptake or a dynamic equilibrium between uptake and regeneration (nitrification) is suggested as

possible explanations for these non-zero nitrate concentrations (EPPLEY *et al.*, 1990; MCCARTHY *et al.*, 1992; HARRISON *et al.*, 1996; DORE and KARL, 1996b). At other stations in the present study, nitrate concentrations in surface waters were higher and more variable, likely reflecting the larger supply of nitrate from depth. Under an assumption of simple one-dimensional diffusion, nitrate supply to the euphotic zone is given by the product of the concentration gradient and vertical diffusivity (KING and DEVOL, 1979). Although the temperature and salinity profiles at Station B were similar to those at Station C (Fig. 4), the nitrate concentration gradient within the nitracline was higher (Fig. 7). At Stations D4, D6, G2, G3 and G6, the mixed layer extended deeper, nearly to the nitracline, which may suggest the entrainment of nitrate from such depths (Figs. 5 and 6). The nitrate

concentration gradient at many of these stations was comparable or higher than at Stations B and C (Fig. 7). Higher concentrations are also reported for “nitrate-depleted” waters in the literature, which may similarly be related to the greater supply of nitrate. At the time-series observation site in the subtropical Atlantic Ocean (BATS), nitrate concentrations in winter were high, sometimes exceeding 300nM (LIPSCHULTZ, 2001). This station is located at a higher latitude (31° 50'N), and winter-mixing extends much deeper than the euphotic zone. The non-winter concentrations of nitrate were similar to those of stratified subtropical waters. Other observations of higher concentrations have been reported for waters associated with mesoscale eddies (GARSIDE, 1985; ALLEN *et al.*, 1996), wind-induced mixing events (EPPLEY and RENGER, 1988; GLOVER *et al.*, 1988), and possible atmospheric deposition (EPPLEY *et al.*, 1990), as well as in waters of coastal/shelf regions with terrestrial influence and/or a shallower nitracline (EPPLEY and RENGER, 1986; WOODWARD and OWENS, 1990; EPPLEY *et al.*, 1990; CHEN *et al.*, 2004).

Vertical profiles near the upper end of the nitracline

GARSIDE (1985) first described the vertical distribution of trace nitrate in waters around a warm-core ring in the North Atlantic Ocean, where it was found that nitrate concentrations increased exponentially with depth from the surface. EPPLEY *et al.* (1990) also observed a similar exponential increase in nitrate at certain stations, although more typically the nitrate concentrations were found to be relatively uniform within the euphotic zone and to increase abruptly near the bottom of the euphotic zone. This type of profile is more common in other observations in the subtropical oligotrophic Atlantic and Pacific oceans (EPPLEY and KOEVE, 1990; DORE and KARL, 1996a; LIPSCHULTZ, 2001; CAVENDER-BARES *et al.*, 2001). The profiles obtained in the present study all exhibited the latter type of distribution. The upper layer (no concentration gradient) and the nitracline layer (positive concentration gradient) can be clearly separated (Fig.

7).

Based on nitrate data obtained by conventional analytical methods in the equatorial Atlantic Ocean, HERBLAND and VOITURIEZ (1979) suggested that the 1% light depth, chlorophyll maximum and upper end of the nitracline all occur at statistically similar depths. Determination of these depths largely depends on the depth intervals of sampling. In the present study, smaller sampling intervals of 5–10m were adopted for nitrate analysis near the depth of the lower euphotic zone, and the results confirmed that the upper end of the nitracline is associated within a narrow relative PAR range of 0.58–3.5%. Stations G2 and G6 are the exception to this behavior (Fig. 8), where the mixed layer extended much deeper than the 1% light depth. The lower relative PAR recorded at the upper end of the nitracline at these two sites (0.30–0.47% for G2, 0.21–0.26% for G6) should thus be representative of the deep mixed layer. Given the association of nitrate uptake with photosynthetic activity, the occurrence of the upper end of nitracline at similar light-depths indicates a strong biological control on the nitrate distribution.

The maintenance of this type of vertical profiles constrains the vertical variation in the nitrate budget. Assuming the simple one-dimensional diffusive supply of nitrate, the

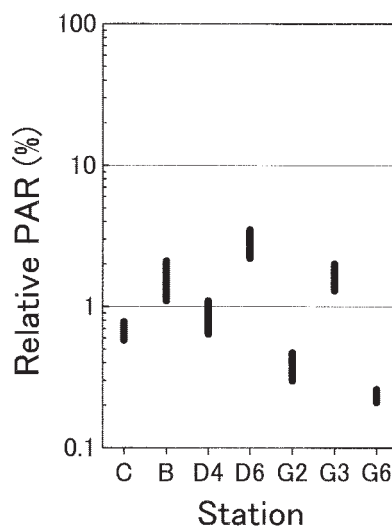


Fig. 8. Estimated depths of upper end of nitracline in terms of relative PAR.

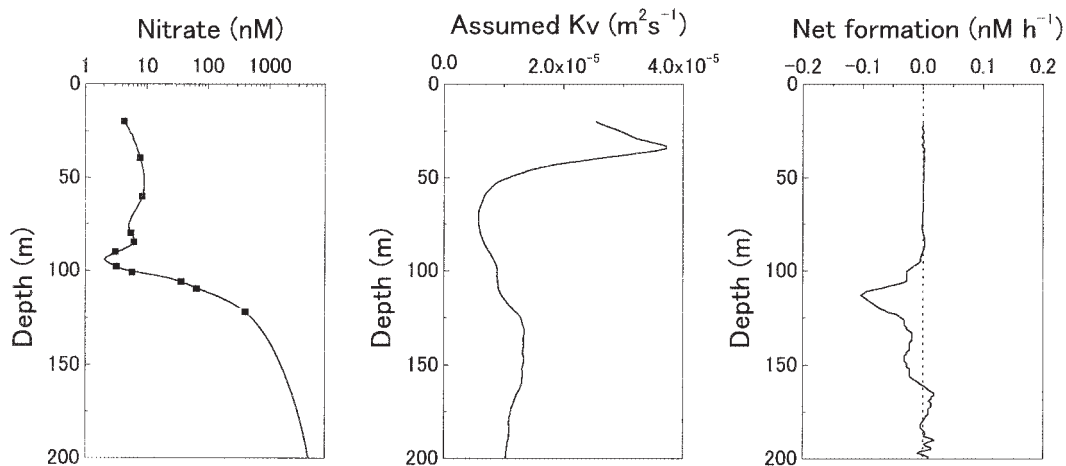


Fig. 9. Interpolated nitrate concentration distribution, assumed vertical diffusivity and estimated net formation/uptake (formation for positive values) of nitrate at Station C.

temporal change of the nitrate concentration (C) at depth z , or the time (t) derivative of C , can be equated with the depth derivatives of C , the vertical diffusivity at depth z [$K_v(z)$] and biological uptake and regeneration of nitrate:

$$\frac{\partial C}{\partial t} = \frac{\partial}{\partial z} \left(K_v(z) \frac{\partial C}{\partial z} \right) - (\text{uptake}) + (\text{regeneration}) \quad (1)$$

The net biological uptake of nitrate, or the negative value of the net biological formation, should be given as the difference between the uptake and regeneration.

$$(\text{net biological uptake}) = -(\text{net biological formation}) = (\text{uptake}) - (\text{regeneration}) \quad (2)$$

If the nitrate concentration is in a steady state, the time derivative of C in Equation (1) equals zero, and the net biological uptake is given as

$$(\text{net biological uptake}) = \frac{\partial}{\partial z} \left(K_v(z) \frac{\partial C}{\partial z} \right) \quad (3)$$

The vertical diffusivity at depth z is assumed to be a function of buoyancy frequency or N (GARGETT 1984) as follows.

$$K_v(z) = a_0 N^{-1} \quad (4)$$

An arbitrary value of $1.0 \times 10^{-7} \text{m}^2 \text{s}^{-1}$ is assigned for the constant a_0 . The resultant vertical distribution of the net biological uptake of

nitrate at Station C (Fig. 9) indicates that high net uptake should occur over a narrow depth range near the upper end of the nitracline, whereas no net uptake or formation should occur in the upper layers of the euphotic zone. If plankton populations in these layers utilize nitrate as a nitrogen source, the uptake of nitrate should be in balance with the *in situ* supply of nitrate, or biological regeneration (presumably nitrification) and/or an alternative external supply such as atmospheric deposition.

Acknowledgements

The authors thank the scientists, officers and crewmembers onboard the relevant cruises of the R/V *Hakuho-maru*, R/V *Tansei-maru* and R/V *Kaiyo*. Field observations onboard R/V *Kaiyo* were conducted as a part of the MASFLEX project. This study was supported by Grants-in-Aid from the Ministry of Education, Culture, Sports, Science and Technology of Japan (Nos. 04232206, 04740355, 05216203, 06740420 and 07640655).

References

- ALLEN, C.B., J. KANDA and E.A. LAWS (1996): New production and photosynthetic rates within and outside a cyclonic mesoscale eddy in the North Pacific subtropical gyre. *Deep-Sea Res. I*, **43**, 917–936.
- CAVENDER-BARES, K.K., D.M. KARL and S.W. CHISHOLM (2001): Nutrient gradients in the western North Atlantic Ocean: Relationship to

- microbial community structure and comparison to patterns in the Pacific Ocean. *Deep-Sea Res. I*, **48**, 2373–2395.
- CHEN, Y.L.L., H.Y. CHEN, D.M. KARL and M. TAKAHASHI (2004): Nitrogen modulates phytoplankton growth in spring in the South China Sea. *Continental Shelf Res.*, **24**, 527–541.
- COX, R.D. (1980): Determination of nitrate and nitrite at the part per billion level by chemiluminescence. *Anal. Chem.*, **52**, 332–335.
- DORE, J.E. and D.M. KARL (1996a): Nitrite distributions and dynamics at Station ALOHA. *Deep-Sea Res. II*, **43**, 385–402.
- DORE, J.E. and D.M. KARL (1996b): Nitrification in the euphotic zone as a source for nitrite, nitrate and nitrous oxide at Station ALOHA. *Limnol. Oceanogr.*, **41**, 1619–1628.
- EPPLEY, R.W., C. GARSIDE, E.H. RENGER and E. ORELLANA (1990): Variability of nitrate concentration in nitrogen-depleted subtropical surface waters. *Mar. Biol.*, **107**, 53–60.
- EPPLEY, R.W. and W. KOEVE (1990): Nitrate use by plankton in the eastern subtropical North Atlantic, March–April 1989. *Limnol. Oceanogr.*, **35**, 1781–1788.
- EPPLEY, R.W. and E.H. RENGER (1986): Nitrate-based primary production in nutrient-depleted surface waters off California. *Oceanographie Tropicale*, **21**, 229–238.
- EPPLEY, R.W. and E.H. RENGER (1988): Nanomolar increase in surface layer nitrate concentration following a small wind event. *Deep-Sea Res.*, **35**, 1119–1125.
- GARGETT, A.E. (1984): Vertical eddy diffusivity in the ocean interior. *J. Mar. Res.*, **42**, 359–393.
- GARSIDE, C. (1982): A chemiluminescent technique for the determination of nanomolar concentrations of nitrate and nitrite in seawater. *Mar. Chem.*, **11**, 159–167.
- GARSIDE, C. (1985): The vertical distribution of nitrate in open ocean surface water. *Deep-Sea Res.*, **32**, 723–732.
- GLOVER, H.E., B.P. PRÉZELIN, L. CAMPBELL, M. WYMAN and C. GARSIDE (1988): A nitrate-dependent bloom in surface Sargasso Sea water. *Nature*, **331**, 161–163.
- HARRISON, W.G., L.R. HARRIS and B.D. IRWIN (1996): The kinetics of nitrogen utilization in the oceanic mixed layer: Nitrate and ammonium interactions at nanomolar concentrations. *Limnol. Oceanogr.*, **41**, 16–32.
- HERBLAND, A. and B. VOITURIEZ (1979): Hydrological structure analysis for estimating the primary production in the tropical Atlantic ocean. *J. Mar. Res.*, **37**, 87–101.
- ISHIMARU, T., H. OTOBE, T. SAINO, H. HASUMOTO and T. NAKAI (1984): OCTOPUS, an octo parameter underwater sensor, for use in biological oceanography studies. *J. Oceanogr. Soc. Japan*, **40**, 207–212.
- KANDA, J., T. ITOH, D. ISHIKAWA and Y. WATANABE (2003): Environmental control of nitrate uptake in the East China Sea. *Deep-Sea Res. II*, **50**, 403–422.
- KARL, D.M. and R. LUKAS (1996): The Hawaii Ocean Time-series (HOT) program: Background, rationale and field implementation. *Deep-Sea Res. II*, **43**, 129–156.
- KING, F.D. and A.H. DEVOL (1979): Estimates of vertical eddy diffusion through the thermocline from phytoplankton nitrate uptake rates in the mixed layer of the eastern tropical Pacific. *Limnol. Oceanogr.*, **24**, 645–651.
- KROM, M.D., E.M.S. WOODWARD, B. HERUT, N. KRESS, P. CARBO, R.F.C. MANTOURA, G. SPYRES, T.F. THINGSTAD, P. WASSMANN, C. WEXELS-RISER, V. KITIDIS, C.S. LAW and G. ZODIATIS (2005): Nutrient cycling in the south east Levantine basin of the eastern Mediterranean: Results from a phosphorus starved system. *Deep-Sea Res. II*, **52**, 2879–2896.
- LETELIER, R.M., D.M. KARL, M.R. ABBOTT, P. FLAMENT, M. FREILICH, R. LUKAS and T. STRUB (2000): The role of late winter meso-scale events in the biogeochemical variability of the upper water column of the North Pacific Subtropical Gyre. *J. Geophys. Res.*, **105**, 28,723–28,739.
- LIPSCHULTZ, F. (2001): A time-series assessment of the nitrogen cycle at BATS. *Deep-Sea Res. II*, **48**, 1897–1924.
- MANTOURA, R.F.C., C.S. LAW, N.J.P. OWENS, P.H. BURKILL, E.M.S. WOODWARD, R.J.M. HOWLAND and C.A. LLEWELLYN (1993): Nitrogen biogeochemical cycling in the northwestern Indian Ocean. *Deep-Sea Res. II*, **40**, 651–671.
- MCCARTHY, J.J., C. GARSIDE and J.L. NEVINS (1992): Nitrate supply and phytoplankton uptake kinetics in the euphotic layer of a Gulf Stream warm-core ring. *Deep-Sea Res.*, **39**, S393–S403.
- OUDOT, C. and Y. MONTEL (1988): A high sensitivity method for the determination of nanomolar concentrations of nitrate and nitrite in seawater with a Technicon AutoAnalyzer II. *Mar. Chem.*, **24**, 239–252.
- STRICKLAND, J.D.H. and T.R. PARSONS (1972): *A Practical Handbook of Sea Water Analysis*, 2nd edition. Bulletin of Fisheries Research Board of Canada, **167**, 1–310.
- TSUNOGAI, S., K. ISEKI, M. KUSAKABE and Y. SAITO (2003): Biogeochemical cycles in the East China Sea: MASFLEX program. *Deep-Sea Res. II*, **50**, 321–326.
- WOODWARD, E.M.S. and N.J.P. OWENS (1990): Nutrient depletion studies in offshore North Sea

areas. Netherlands J. Sea Res., **25**, 57–63.

ZHANG, J.-Z. (2000): Shipboard automated determination of trace concentrations of nitrite and nitrate in oligotrophic water by gas-segmented continuous flow analysis with a liquid waveguide

capillary flow cell. Deep-Sea Res. I, **47**, 1157–1171.

Received June 8, 2007
Accepted July 9, 2007